Desalination and Water Treatment
www.deswater.com

doi: 10.1080/19443994.2013.839400

53 (2015) 73–83
January

Taylor & Francis
Taylor & Francis Group

Effect of air sparging on flux enhancement during tangential flow filtration of degreasing effluent

Prabhavathy Sivaprakash[a,*], Sunando DasGupta[b]

[a]*Process Plant Engineering, CSIR-Central Mechanical Engineering Research Institute, Mahatma Gandhi Avenue, Durgapur 713209, India*
Tel. +91 343 6452206; email: cprabhavathy@gmail.com
[b]*Department of Chemical Engineering, Indian Institute of Technology Kharagpur, Kharagpur 721302, India*

Received 7 April 2013; Accepted 14 August 2013

ABSTRACT

The favorable effects of air sparging to reduce deposition on the membrane and consequent fouling during membrane separation are studied, first with a model solute (pectin), followed by degreasing effluent from a tannery. Directly injecting air into the feed stream enhances the permeate flux and the performance of the separation process in a rectangular flat sheet tangential flow membrane module. The effects of various operating parameters, namely, gas velocity, membrane surface orientations with respect to the flow direction, transmembrane pressure, cross-flow velocity, and model solute concentration, are quantified. The concentrations of pectin solutions used herein are chosen such that they behave similar to the degreasing effluent in terms of gel layer-type deposition on the membrane surface. Also, there are significant changes in the permeate quality (80 mg/l) by using air sparging in the flow channel which is below Indian discharge standards (250 mg/l). There are appreciable changes in the permeate quality when air sparging is employed compared to membrane separation without aeration. Image analyzing video microscopy is effectively used to precisely measure variation in deposition thicknesses on surface of the membrane as functions of operating parameters. Once the effectiveness of the method is established, the technique is successfully used, with significant flux enhancement, to treat degreasing effluent from a tannery.

Keywords: Air sparging; Membrane fouling; Deposition thickness; Flux enhancement; Degreasing effluent

1. Introduction

Membrane filtration has increasingly become an important technology for separation in a number of industrial processes. Concentration polarization and fouling of membranes are major problems that need consideration [1]. One of the meaningful approaches to alleviate these limitations is to alter the flow hydrodynamics. Pressure-driven membrane-based separation processes are used for separation in extensively varying industrial processes which include bio-separation, chemical industries, dairy, food processing, petrochemicals, pulp and paper, sugar, tannery, textiles, etc. [2,3]. Low energy requirement, unique separation potential, concentration and separation achieved without change of phase, ease of

*Corresponding author.

scaling-up, etc. are few advantages of membrane technology. Familiar limitations during operation in membrane-based separation processes include concentration polarization and membrane fouling [4,5]. According to Seminario et al. [6], a concentration boundary layer develops during membrane separation, leading to accumulation of solutes near the membrane surface called concentration polarization, thereby causing fouling on the membrane material as well as adsorption inside the pores leading to pore blocking. A gel with stable gel concentration may appear on the membrane surface when protein molecules are used, due to the fact that bulk concentration of higher molecular weight solute is much less than that of the gel layer concentration. A concentration boundary layer forms from the bulk of the solution up to the gel layer. Gel layer development hampers permeate flow, in addition to that of membrane hydraulic resistance.

Flux-reducing effects can be reduced to a certain level but cannot be avoided. Extensive research has been carried out to improve the permeate flux. Some of the flux enhancement techniques are: (i) hydrodynamic modification and use of turbulent promoters to improve mass transfer [7], unsteady flows [8], spacers, back flushing, and cleaning, which lead to flux improvement [9]; (ii) addition of air/gas to the liquid stream to increase turbulence near the surface of the membrane thereby suppressing boundary layer formation [10,11]; (iii) vibration of flat sheet reverse osmosis membrane to reduce fouling [12]; (iv) application of external body force such as dc electric field [13] and magnetic field; and (v) modification of membrane surface, e.g. by plasma treatment to reduce fouling [14].

The concept that gas–liquid two-phase flow generated by injecting air bubbles along with the feed can result in substantial improvement of permeate flux has been studied in the past [15–17]. Gas bubbles have the added advantage of easy separation with considerable permeate flux enhancement from the retentate stream and aid in separation [18,19]. Addition of air to the liquid stream increases turbulence near the membrane surface which suppresses the formation of concentration boundary layer, leading to flux enhancement [20]. Using this technique, Cui et al. [10,21] have reported a 250% improvement in flux compared to conventional cross-flow operation for ultrafiltration (UF) of dyed dextran solution. In an excellent review article, Cui et al. has focused on the use of gas bubbles and slugs in tubular and hollow fiber membranes and channels containing flat sheets. Different gas–liquid two-phase flow patterns are described and air bubbling and other factors that influence the phenomena of flux enhancement have been probed in detail [22,23]. Gas bubble-enhanced membrane processing has been applied to membrane bioreactor, hybrid membrane processes for surface water polishing, bioprocesses separations, and cell harvesting [4]. Experimental studies conducted so far aim to improve knowledge of the gas-sparged hollow fiber ultrafiltration membrane (HF UF) process with the ultimate goal of process optimization, through experiments with precisely controlled flow distribution and well-characterized hydrodynamic conditions. It was observed that gas sparging in HF UF membrane systems can increase the permeate flux up to 102% [24]. Lee et al. [25] have also reported the use of air slugs to improve the cross-flow filtration of bacterial suspensions.

In the present study, the effect of body forces on flux enhancement during air sparging in a flat sheet module has been investigated in detail. It has been found that introduction of gas–liquid two-phase flow significantly enhances the system performance since orientation [26] plays an important role in flux enhancement. The results of air-sparging-assisted membrane separation of model solute pectin and the effects of various operating parameters are described first, followed by treatment of degreasing effluent both in presence and absence of air sparging. The beneficial effects of air sparging (in terms of flux improvement) during the treatment of degreasing effluent have been established. The air slugs are forced to abrade the membrane surface, arresting the development of the concentration boundary layer and reducing the establishment of a gel layer deposition on the membrane surface.

2. Experimental

2.1. Materials

Flat sheet poly phenylene ether sulfone membrane of molecular weight cut-off (MWCO) 30 kDa is used for UF. The model solute used for UF is pectin (molecular weight 30,000–100,000 and degree of esterification 63–66%) supplied from Loba-Chemie, India. For experiments with the industrial effluent, organic thin film composite membrane with MWCO 400 Da is used for nanofiltration (NF). The industrial effluent used for NF study was collected from the degreasing unit of M/s, Olympic Tannery, Banthala Leather complex, Kolkata, India [27]. Commercial-grade alum is used in the degreasing effluent for coagulation. The chemicals required for determination of chemical oxygen demand (COD) are procured from M/s, Loba Chemie, India.

2.2. Pretreatment

2.2.1. Pretreatment of the effluent

A pretreatment procedure is essential to lessen the excess load on the membrane system due to the fact that huge quantities of suspended materials are present floating or dissolved in the effluent. Herein, for degreasing effluent, different doses of alum were used for pretreatment. By adding different alum doses to the effluent which ranges from 0.1 to 0.8 g/l in eight 100 ml capacity cylinders undergoes vigorous mixing and allowed to settle for 30 min after which pH, COD, total solids (TSs), total dissolved solids (TDS) and conductivity are measured. The optimum coagulant dosage in this case is 0.7 g/l as the COD range at this condition is the lowest (734 mg/l). The supernatant is siphoned out for conducting further experiments leaving the sludge that is settled at the bottom.

2.3. Analysis

The conductivity, TDS, TS, COD, and pH of all samples (feed, permeate, and retentate streams) are measured after each experiment. Conductivity and TDS were measured using a water and soil analysis kit, model no 191E, manufactured by M/s, Toshniwal Instruments Ltd, India. pH of the sample is measured by a pH meter, supplied by Toshniwal Instruments, India. TSs of samples are calculated by taking 5 ml of sample in a petridish and introducing it in an oven set aside at 105 ± 2°C until entire sample is dried. COD values (gravimetric analysis) are determined using a standard procedure [28].

2.4. Membrane cell with air-sparging setup

The experimental setup is a fabricated stainless steel rectangular cross-flow cell. The schematic diagram of the experimental setup is shown in Fig. 1. The membrane cell consists of two rectangular analogous flanges as presented in Fig. 2. The top and bottom flanges are mirror-polished and grooved, forming the permeate flow channel. A porous stainless steel laminate present on the bottom flange provides mechanical support to the membrane over which two neoprene rubber gaskets are placed. Then, two flanges are assembled together to form a leak proof channel for conducting experiments in cross-flow mode. For experiments with air sparging, air is injected from a pressurized cylinder through a gas rotameter to the membrane cell along with the feed. Two non-return valves prevent backflow of gas.

The feed (pectin solute) from the feed tank is pumped to the cross-flow cell by a high pressure reciprocating pump. The cell consists of two rectangular matching flanges with mirror-polished top flange and grooved bottom flange forming the channels for the permeate flow. The effective length, width, and surface area of the membrane is 14.6×10^{-2} m, 5.5×10^{-2} m, and 8.03×10^{-3} m^2. The channel height after tightening the two flanges is found to be 3.4×10^{-3} m [27]. The liquid flow rate is measured by a rotameter in the retentate line. The air introduced in the membrane cell along with the feed liquid creates turbulence in the flow path. Pressure inside the air-sparged membrane cell is controlled by a bypass valve. To measure permeate flux and concentration, known volume of permeate samples is collected from the bottom side of the membrane cell assembly.

2.5. Experimental design

The aim of the present study is to investigate the useful effects of air sparging, first using model solute pectin and then using experiments that are conducted with an actual industrial effluent. UF experiments with pectin are designed to observe the effects of variation in operating conditions such as pressure, liquid flow rate, gas flow rate, inclination, feed concentration, etc. The operating variables used in this experiment are pressures (207, 276, 414, and 552 kPa), a constant liquid flow rate (90 L/h), gas flow rates (10, 20 and 30 L/h), and feed compositions (0.1% pectin, 0.2% pectin, and 0.4% pectin). Optical quantification of thickness of the gel layer deposition on the membrane surface under different operating conditions is also performed. In case of NF of degreasing effluent, the operating variables used are pressure (828 kPa), liquid flow rate (90 L/h), and gas flow rates (10, 20, and 30 L/h). The membrane permeability (L_p) of UF and NF membrane is found to be 1×10^{-10} m/Pa.s and 2.84×10^{-11} m/Pa.s, respectively. Air sparging does not influence the pure water permeability of membranes.

2.6. Experimental procedure

The clarified supernatant collected after gravity settling is used as a feed for conducting experiments. The feed tank (stainless steel with 2 L volume) holds the feed solution. This feed is pumped to the cross-flow membrane cell by means of a high pressure reciprocating pump. Permeate is collected

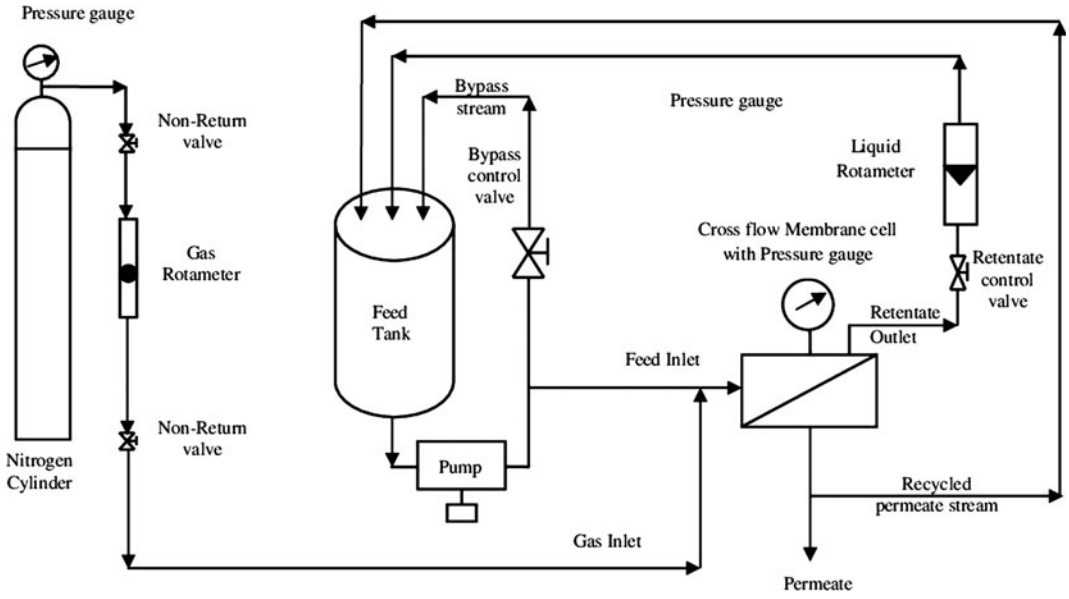

Fig. 1. Schematic of air-sparging experimental setup.

during experiments at different time period for further analysis. To retain constant concentration in the feed tank, permeate is recycled to the feed tank. To vary the pressure and flow rate independently, retentate and bypass control valves are provided. From the slopes of cumulative volume vs. time plot, the permeate flux values are determined. The accuracy of flux amount measured is within ± 5%. Experiments are conducted at ambient temperature. Distilled water is used to wash the membrane *in situ* once experiments are completed. After meticulous membrane cleaning, the cross-flow cell is reassembled and the membrane permeability is measured. It is observed that permeability remains nearly constant between successive runs.

2.7. Details of deposition thickness and optical studies

Deposition thickness is a measure of solute buildup and therefore enhanced resistance to flow through the membrane on the membrane surface during cross-flow filtration. After UF experiments with pectin, the filtration chamber is opened and the membrane along with the deposition over it is vacuum-dried in presence of diphosphorous pentoxide (P_2O_5) for two hours using the methodology described in [29]. The dehydrated membranes are cut cautiously for sampling and fragmented into 4 mm × 3 mm size. Every cut sample strip is set perpendicularly with its edging apprehended up at the rim of a glass slide. The glass slide with jut sample piece is positioned underneath an image resolution visual microscope. High resolution image-analyzing video microscopy is used to accurately quantify the change in deposition thicknesses on the membrane surface as functions of operating parameters. Several images at different locations are acquired on top view of the membrane protruded piece which is further examined to determine deposition. In order to take into account local variations, images are captured at a number of points for each such membrane piece and average. The membrane sampling along with the deposited layer is done carefully so as to include the complete area. The images are examined to assess the deposition thickness above the membrane face. "Image-Pro Plus", image-processing software is used to determine the deposition thickness. Each experimental points reported in this study are averaged over 8–10 measurements. The average thickness of the synthetic support zone is about 120 μm and the same of the polymer zone is 60 μm.

3. Results and discussion

Effects of various operating parameters on the performance of the process are studied. The scheme is first tested with a model solute (pectin) and later the technique is used to treat an industrial effluent, namely degreasing effluent from a tannery. Pectin is chosen as the standard model solute as it has a tendency to form gel-type layer on the membrane surface, which is fundamentally similar to that

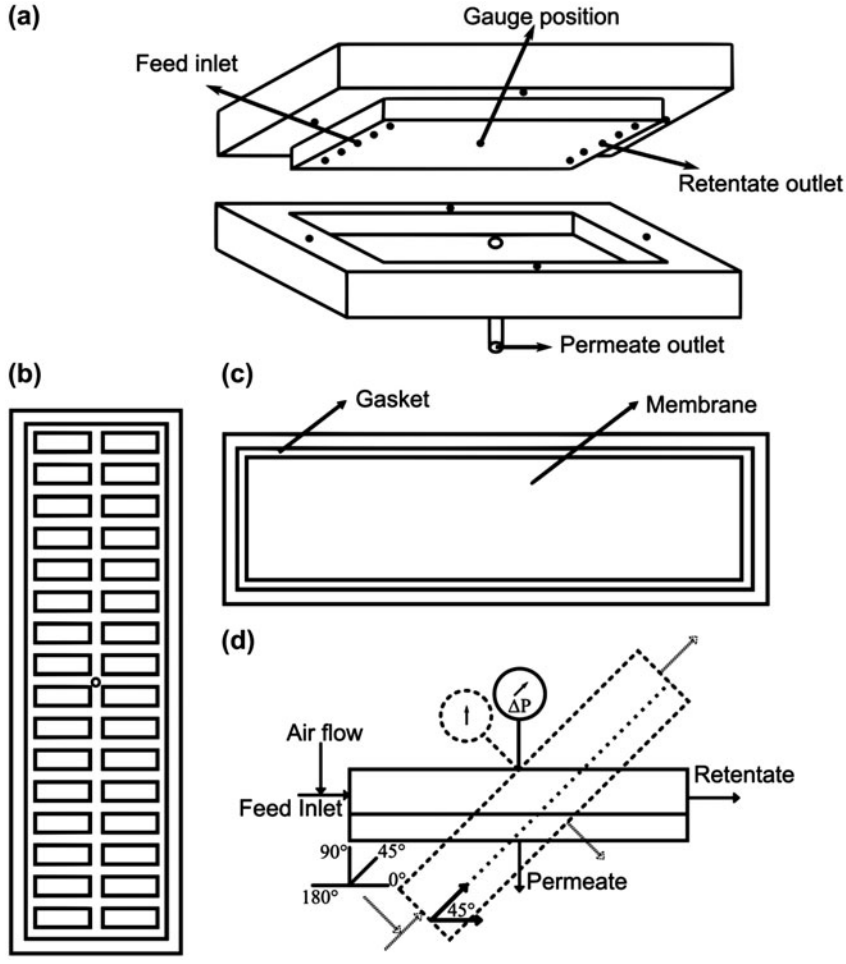

Fig. 2. Cross-flow membrane module assembly: (a) open view of top and bottom flange, (b) bottom flange with grooves, (c) membrane and gasket positioned above the bottom flange, and (d) membrane orientation (0° and 45°).

observed during the treatment of degreasing effluent. Since pectin solutions are relatively easy to handle (the deposited layers are easy to clean), the proof of concept and the parametric studies are performed with pectin and finally with the degreasing effluent from a tannery. The effect of aeration will be more clear if the deposition pattern of model solutes (pectin) and an industrial effluent can be accurately measured after the experiments as functions of various operating parameters including the change in inclinations of the experimental system (causing appreciable changes in the flow pattern near the membrane surface) and gas flow rates vis-à-vis the liquid flow rates.

3.1. Effect of gas flow rate on permeate flux and deposition thickness

The influence of gas flow rate on UF using pectin is investigated at a liquid velocity of 90 L/h and at an inclination angle of zero degrees ($\theta = 0^{\circ}$) with respect to the horizontal, at 0.2% pectin concentration with a transmembrane pressure of 276 kPa. The results are presented in Fig. 3. The standard deviations of the measurements for each of reported data are calculated. Standard error bars, estimating certainty of the mean, are included in figures which is less than ±0.5. It can be seen from the figure that as the gas flow rate increases, deposition thickness decreases and permeate flux increases for a constant inclination and liquid flow rate. The injection of air increases the turbulence and leads to reduction in concentration polarization. Similar observations are made by other researchers using a number of solutes (BSA, Dextran, and Lysozyme) [10,21]. Aeration of gas bubbles assists in substantial flux improvement without affecting the membrane material [17]. The flow of gas slugs or bubbles arrests the growth of the concentration polarization layer, thereby reducing the deposition of pectin

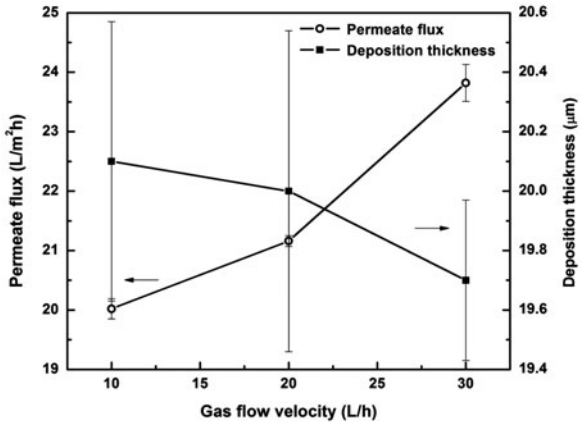

Fig. 3. Effect of permeate flux and deposition thickness on gas flow rate (constant operating pressure—276 kPa, liquid flow rate—90 L/h, and feed concentration—0.2% pectin).

molecules on the membrane surface and reducing the overall resistance to permeate flow through the membrane [30]. The corroboration between the deposition profiles and the enhancement of permeate flux is explored and the experimental results are found to be consistent with the physics of the process. The effect becomes more pronounced at higher gas flow rates resulting in significant flux enhancement. The flux enhancements achieved for 10, 20, and 30 L/h of gas flow rate are 7, 12, and 22%, respectively.

3.2. Variation of permeate flux and deposition thickness with different membrane orientations

It has been postulated that the gravity field will substantially alter the shape and size of the bubbles near the membrane surface leading to varying degrees of turbulence and flux enhancement [31]. The relatively higher values of transmembrane pressure (276 kPa for this set of experiments) preclude the use of a transparent material as the material of construction for the membrane cell and hence the movement of gas slugs with the feed through the membrane channel cannot be viewed. Therefore, an alternative method of indirectly quantifying the effects of the gas sparging velocity, namely the measurement of deposition thickness after a set of experiments, has been used in this study using a technique already developed [32]. The variations in deposition thickness and permeate flux under different membrane orientations (0˚, 45˚, 90˚, and 180˚) at a constant feed concentration, pressure, liquid, and gas flow rates of 0.2% pectin, 276 kPa, 90 L/h, and 30 L/h, respectively are presented in Figs. 4 and 5. The deposition thickness decreases significantly with change in angle of inclination of the membrane setup as shown in Fig. 4(a)–(d). Membrane skin, support, and solute deposition are shown in Fig. 4(e). Deposition thickness measurement technique: L1 is drawn for demarcation of the top of the deposition layer; L2 is drawn at the interface of the deposition layer and top of the membrane surface; and L3 to L10 are drawn to measure the deposition thickness. For each such mounted membranes, images are captured at different locations and averaged to take in account local fluctuations. The cross-sections of the sample pieces cut from the relevant locations of the membranes are analyzed under a camera-interfaced optical microscope. As membrane orientation angle increases from 0˚ to 180˚, the average deposition thickness decreases from 19.7 to 14.6 μm as can be seen in Fig. 5. This has led to substantial decrease in the resistance to the flow through the membrane and the permeate flux increases appreciably.

A change in inclination from 0˚ to 180˚ has resulted in an increase of permeate flux from 23.8 to 30.6 L/m^2h i.e. an increase of 22–39%. The effects of inclination of the flow chamber and the gas flow rate are found to be significant with respect to flux enhancement. The system is inclined with respect to the horizontal, the bubbles flowing with the feed move closer to the membrane surface causing greater turbulence and lesser deposition. The effect is the maximum when the system is rotated by an angle of 180˚ so that the bubbles traveling with the feed solution graze past the membrane surface due to buoyancy and minimizes the thickness of the deposited layer. The effects of other operational parameters, such as transmembrane pressure drop, feed concentration, liquid, and gas flow rates on permeate flux, are discussed in the following sections.

3.3. Effect of permeate flux and deposition thickness with transmembrane pressure drop

Increase in transmembrane pressure increases the magnitude of the permeate flux, due to larger driving force, as shown in Fig. 6. For a constant pectin concentration (0.2% pectin), liquid flow rate is 90 L/h; gas flow rate is 30 L/h; and the steady state permeate flux values are 22.8, 26.5, 31.2, and 35.4 L/m^2h for 207, 276, 414, and 552 kPa of pressures, respectively. However, the increase in transmembrane pressure and the enhanced convective flow towards the membrane surface enhance the formation of gel-type layer on the membrane surface. For example, as transmembrane pressure increases from 207 to 552 kPa, the deposition thickness increases from 11.3 to 15.6 μm. This provides additional resistance to permeate flow, in series to that of the hydraulic resistance of the membrane.

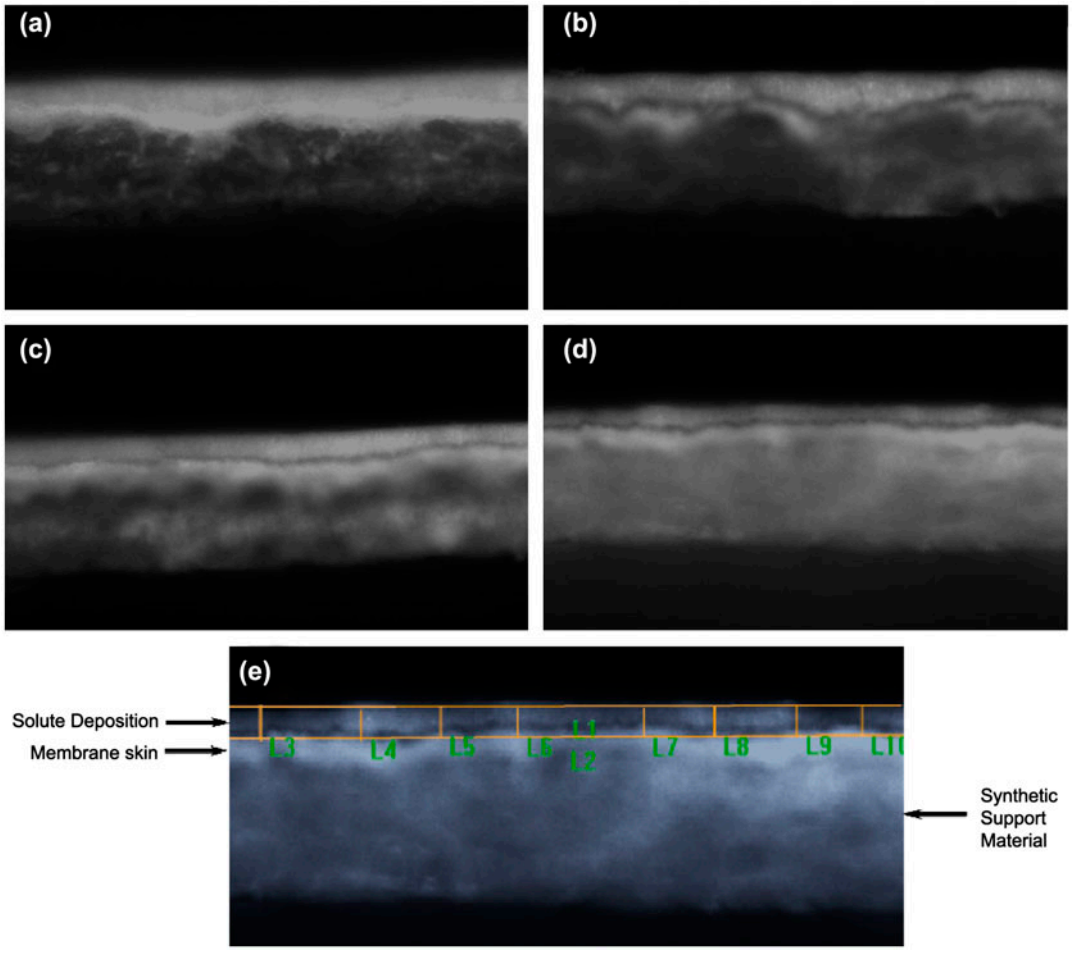

Fig. 4. Reduction in deposition thickness with orientations of (a) $\theta = 0^{\circ}$, (b) $\theta = 45^{\circ}$, (c) $\theta = 90^{\circ}$, (d) $\theta = 180^{\circ}$, and (e) deposition thickness measurement of the solute layer over the membrane surface.

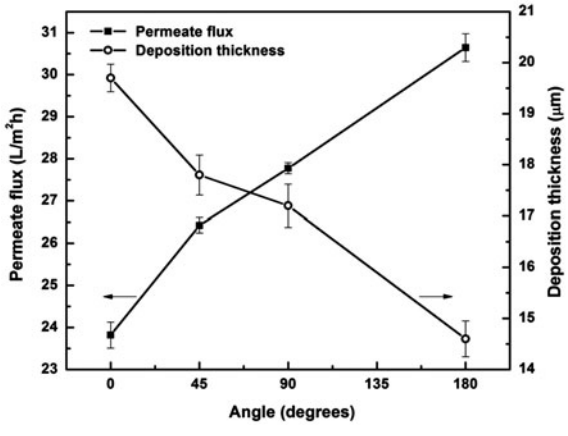

Fig. 5. Variation of permeate flux and deposition thickness with different membrane orientations (constant operating pressure—276 kPa, liquid flow rate—90 L/h, gas flow rate—30 L/h, and feed concentration—0.2% pectin).

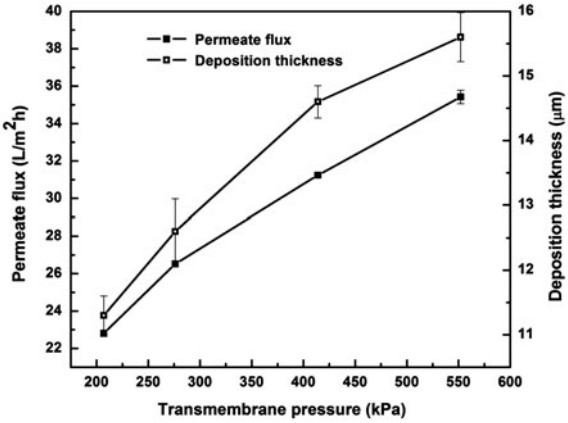

Fig. 6. Variation of permeate flux with transmembrane pressure (constant liquid flow rate—90 L/h, gas flow rate—30 L/h, and feed concentration—0.2% pectin).

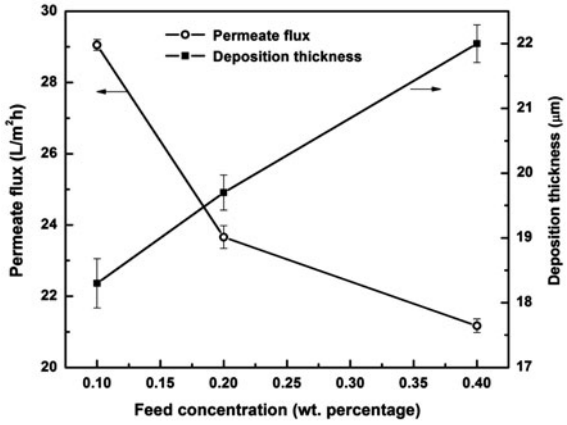

Fig. 7. Variation of deposition thickness and permeate flux with feed concentration (constant operating pressure—276 kPa, liquid flow rate—90 L/h, and gas flow rate—30 L/h).

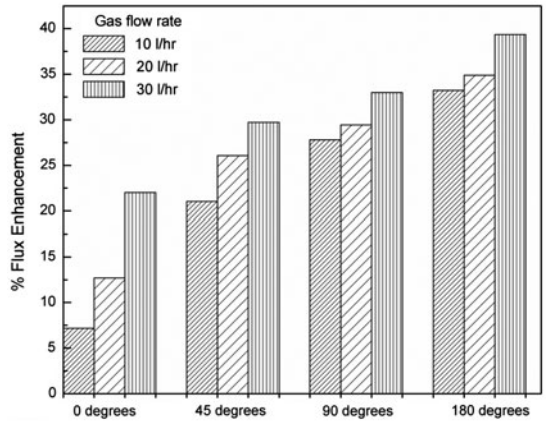

Fig. 8. Effect of flux enhancement during ultrafiltration of pectin (constant operating pressure—276 kPa, liquid flow rate—90 L/h, and feed concentration—0.2% pectin).

However, the associated increase in resistance to flow is more than compensated by the additional transmembrane pressure drop and the overall permeate flux increases.

3.4. Variation of deposition thickness and permeate flux with concentration of the solution and cross-flow velocity

The effects of feed concentration on permeate flux and deposition thickness are shown in Fig. 7. Higher concentration of pectin in the feed solution leads to more deposition of solute particles on the membrane surface resulting in an increase in the deposition thickness and a consequent reduction of the effective driving force for solvent flow. The experimental permeate flux decreases substantially with an increase in solute concentration. For example, the permeate fluxes for 0.1, 0.2, and 0.4% pectin concentration are 29.1, 23.6, and 21.2 L/m^{2}h, respectively. The corresponding deposition thickness increases from 18.3 to 22 μm keeping other parameters constant (liquid flow rate, gas flow rate, and transmembrane pressure at 90 L/h, 30 L/h, and 276 kPa, respectively). The increased shearing action of faster moving liquid over the membrane surface leads to a decrease in deposition and results in flux increase. Flux enhancement of around 14–26% is achieved when the cross-flow velocity is increased from 60 to 120 L/h. The optically measured deposition thickness decreases from 23.2 to 18.2 μm, when the cross-flow velocity is increased from 60 to120 L/h.

3.5. Flux enhancement during UF of Pectin

One of the major emphasis of this study is to probe the effect of orientation of the flow channel on permeate flux enhancement using air sparging to generate two-phase cross-flow in order to overcome (at least partially) concentration polarization in membrane separation. The effects of another important operating variable, namely, the gas flow rates, have also been studied. The results of these experiments with the model solute pectin are summarized in Fig. 8 at a constant pressure and liquid flow rate of 276 kPa and 90 L/h, respectively. Three gas flow rates are used, namely, 10, 20, and 30 L/h and the angles are varied from the horizontal (0˚) to 45˚, vertical to 90˚, and inverted to 180˚. It is clear from the figure that significant flux enhancement to the tune of more than 30% can be achieved even at a low air-sparging rate (10 L/h) if the membrane cell is oriented favorably ($\theta = 90^\circ$). The effect is most pronounced for an inclination of 180˚ for reasons already discussed; however, it is important to note that orientation effect is much

Table 1
Characterization of degreasing effluent

Influent properties	pH	Conductivity (S/m)	TS (g/l)	TDS (g/l)	COD (mg/l)
Feed (degreasing effluent)	8.6	2.6	31.3	17.5	3,737
After alum dose 0.7%,w/v	7.1	2.9	27.4	19.1	734

Table 2
Permeate properties after membrane filtration [828 kPa pressure and 90 L/h effluent flow rate]

Permeate properties after NF (by varying flow dynamics)	pH	Conductivity (S/m)	TS (g/l)	TDS (g/l)	COD (mg/l)
In absence of air sparging	7.8	14.9	12.7	9.9	125
In presence of air sparging [10 L/h gas flow rate]	7.3	10.1	2.0	6.1	80

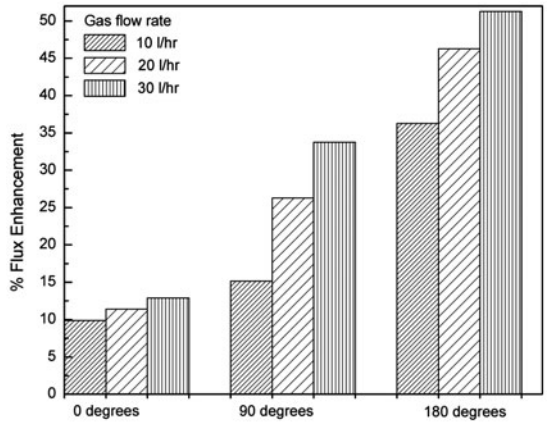

Fig. 9. Flux enhancement during air-sparging-assisted membrane separation of degreasing effluent (constant operating pressure—828 kPa, liquid flow rate—90 L/h, and feed used in this case is degreasing effluent with unknown concentration).

more significant than the enhancement caused by increase in gas flow rate with inclination angle equal or above 90°. Based on these above investigations, similar approach is adopted for a common industrial effluent—the degreasing effluent from tannery that has a large amount of suspended solids which poses significant problems during treatment using membrane separation.

3.6. Air sparging during NF of degreasing effluent

Degreasing effluent from a tannery is treated first using a coagulation process with commercially available alum as the coagulant, followed by a single-step membrane separation (NF) process in continuous cross-flow mode. The properties of the feed and effluent after alum dosing are presented in Table 1 [27]. As can be seen from the table, the high TS values can cause significant problems of clogging of membrane pores and deposition on the membrane surface thereby decreasing the permeate flux. Therefore, the technique of air sparging to enhance permeate flux is used during cross-flow NF of pretreated degreasing effluent to assess the efficacy of this technique for an industrial effluent. Permeate properties following NF in presence and absence of air sparging in the flow channel are provided in Table 2. NF membranes with MWCO of 400 are used and the experiments are conducted at 828 kPa at a constant liquid flow rate of 90 L/h and varying gas flow rates (10, 20, 30 L/h) and orientations ($\theta = 0^\circ$, 45°, 90°, and 180°). The results are presented in Fig. 9. In line to the results obtained in UF experiments for the model solute pectin, significant flux enhancement to the tune of 50% is achieved when the orientation is 180° in NF experiments. Flux enhancement values reported in Fig. 9 are compared to the flux obtained during NF of 400 Da membrane at 828 kPa and at a constant liquid flow rate of 90 L/h in absence of gas flow rate. The degreasing effluent contains very high COD of 3737 mg/l, but permissible limit is 250 mg/l in India. There are appreciable changes in the permeate quality when air sparging is employed compared to membrane separation without air sparging. For example, the TS, TDS, and the COD values are significantly lower in the previous case (with air sparging). This is due to the fact that with air sparging, the membrane surface concentration reduces as a result of turbulence created by the gas slugs near the membrane surface. Permeate quality improves because reduction in membrane surface concentration leads to decrease of ionic diffusion and leakage. The technique involving air sparging with proper orientation of the membrane setup to force the air-slugs scrape past the membrane surface provides major advantage in case of effluents with high TS and TDS content, which would otherwise rapidly clog the membrane and would result in considerable flux decline. Thus, proper use of air sparging may reduce the need for more frequent cleaning and increases the service life of the membrane. In a related experiment, turbulence promoters are strategically placed in the flow path over the membrane surface but without air sparging, and the increases in the permeate fluxes are quantified. It has been found that under similar conditions, the increases are approximately 5% as compared to the air-sparging enhancements (e.g. 15–20%).

4. Conclusion

The beneficial effects of air sparging during membrane separation is applied for a complex effluent

generated from a tannery containing suspended and dissolved solids. A series of experiments during UF of a model solute (pectin) under various operating conditions of gas flow rate, orientation of the membrane setup, transmembrane pressure, feed concentration, and cross-flow velocity are conducted to gain valuable insights process into the separation. It has been found that the orientation plays an important role in flux enhancement as the air slugs are forced to scrape past the membrane surface, thereby creating additional turbulence and arresting the growth of the concentration boundary layer. This reduces the formation of gel-type layers of rejected solutes on the membrane surface. The thickness of deposited layer has been accurately measured using image analysis and the measurements are consistent with the physics of the process. As membrane orientation angle increases from 0˚ to 180˚ (as shown in Fig. 2), the average deposition thickness decreases from 19.7 to 14.6 μm and results in an increase of permeate flux from 23.8 to 30.6 L/m^2 h i.e. an increase from 22 to 39%. The concept has been used to alleviate the problems commonly associated with industrial effluent with high TS, TDS, and COD that generally results in drastic flux reduction. Processing of degreasing effluent from the leather industry, aided by air sparging, has resulted in significant flux enhancements, to the tune of 30–50% for inclinations of 90^o and 180^o, respectively.

Nomenclature

BSA	—	Bovine serum albumin
COD	—	chemical oxygen demand (mg/l)
HFUF	—	hollow fiber ultrafiltration membrane
L_p	—	membrane permeability (m/Pas)
MBR	—	membrane bioreactor
MWCO	—	molecular weight cut-off (Da)
NF	—	nanofiltration
PES	—	poly ether sulfone
TFC	—	thin film composite
TDS	—	total dissolved solids (g/l)
TS	—	total solids (g/l)
TMP	—	transmembrane pressure (Pa)
UF	—	ultrafiltration
pH	—	hydrogen ion concentration
θ	—	angle (˚)
J	—	permeate flux (m^3/m^2s), (L/m^2h)
μm	—	micron

References

[1] H.C. Van der Horst, J.M.K. Timmer, T. Robbertsen, J. Leenders, Use of nanofiltration for concentration and demineralization in the dairy industry: Model for mass transport, J. Membr. Sci. 104 (1995) 205–218.

[2] B. Van Der Bruggen, C. Vandecasteele, T. Van Gestel, W. Doyen, R. Leysen, A review of pressure-driven membrane processes in wastewater treatment and drinking water production, Environ. Prog. 22 (2003) 46–56.

[3] H. Fadaei, S.R. Tabaei, R. Roostaazad, Comparative assessment of the efficiencies of gas sparging and back-flushing to improve yeast microfiltration using tubular ceramic membranes, Desalination 217 (2007) 93–99.

[4] H. Azami, M.H. Sarrafzadeh, M.R. Mehrnia, Fouling in membrane bioreactors with various concentrations of dead cells, Desalination 278 (2011) 373–380.

[5] G. Schulz, S. Ripperger, Concentration polarization in crossflow microfiltration, J. Membr. Sci. 40 (1989) 173–187.

[6] L. Seminario, R. Rozas, R. Bórquez, P.G. Toledo, Pore blocking and permeability reduction in cross-flow microfiltration, J. Membr. Sci. 209 (2002) 121–142.

[7] C. Prabhavathy, S. De, Estimation of transport parameters during ultrafiltration of pickling effluent from a tannery, Sep. Sci. Technol. 45 (2009) 11–20.

[8] M. Mercier-Bonin, I. Daubert, D. Léonard, C. Maranges, C. Fonade, C. Lafforgue, How unsteady filtration conditions can improve the process efficiency during cell cultures in membrane bioreactors, Sep. Purif. Technol. 22–23 (2001) 601–615.

[9] R. Liikanen, J. Yli-Kuivila, R. Laukkanen, Efficiency of various chemical cleanings for nanofiltration membrane fouled by conventionally-treated surface water, J. Membr. Sci. 195 (2002) 265–276.

[10] Z.F. Cui, K.I.T. Wright, Flux enhancements with gas sparging in downwards crossflow ultrafiltration: Performance and mechanism, J. Membr. Sci. 117 (1996) 109–116.

[11] T.M. Qaisrani, W.M. Samhaber, Impact of gas bubbling and backflushing on fouling control and membrane cleaning, Desalination 266 (2011) 154–161.

[12] M. Gironès i Nogué, I.J. Akbarsyah, L.A.M. Bolhuis-Versteeg, R.G.H. Lammertink, M. Wessling, Vibrating polymeric microsieves: Antifouling strategies for microfiltration, J. Membr. Sci. 285 (2006) 323–333.

[13] B. Sarkar, S. De, Electric field enhanced gel controlled cross-flow ultrafiltration under turbulent flow conditions, Sep. Purif. Technol. 74 (2010) 73–82.

[14] N. Saxena, C. Prabhavathy, S. De, S. DasGupta, Flux enhancement by argon–oxygen plasma treatment of polyethersulfone membranes, Sep. Purif. Technol. 70 (2009) 160–165.

[15] M. Mercier-Bonin, G. Gésan-Guiziou, C. Fonade, Application of gas/liquid two-phase flows during crossflow microfiltration of skimmed milk under constant transmembrane pressure conditions, J. Membr. Sci. 218 (2003) 93–105.

[16] C. Cabassud, S. Laborie, L. Durand-Bourlier, J. Lainé, Air sparging in ultrafiltration hollow fibers: relationship between flux enhancement, cake characteristics and hydrodynamic parameters, J. Membr. Sci. 181 (2001) 57–69.

[17] B.G. Fulton, J. Redwood, M. Tourais, P.R. Bérubé, Distribution of surface shear forces and bubble characteristics in full-scale gas sparged submerged hollow fiber membrane modules, Desalination 281 (2011) 128–141.

[18] A. Drews, H. Prieske, E.-L. Meyer, G. Senger, M. Kraume, Advantageous and detrimental effects of air sparging in membrane filtration: Bubble movement, exerted shear and particle classification, Desalination 250 (2010) 1083–1086.

[19] S. Judd, The MBR Book: Principles and Applications of Membrane Bioreactors for Water and Wastewater Treatment, Elsevier, Oxford, 2010.

[20] P. Willems, A.J.B. Kemperman, R.G.H. Lammertink, M. Wessling, M. van Sint Annaland, N.G. Deen, J.A.M. Kuipers, W.G.J. van der Meer, Bubbles in spacers: Direct observation of bubble behavior in spacer filled membrane channels, J. Membr. Sci. 333 (2009) 38–44.

[21] Z.F. Cui, K.I.T. Wright, Gas—Liquid two-phase cross-flow ultrafiltration of BSA and dextran solutions, J. Membr. Sci. 90 (1994) 183–189.

[22] Z. Cui, S. Chang, A. Fane, The use of gas bubbling to enhance membrane processes, J. Membr. Sci. 221 (2003) 1–35.
[23] A. Laorko, Z. Li, S. Tongchitpakdee, W. Youravong, Effect of gas sparging on flux enhancement and phytochemical properties of clarified pineapple juice by microfiltration, Sep. Purif. Technol. 80 (2011) 445–451.
[24] S.R. Smith, Z.F. Cui, Gas-slug enhanced hollow fibre ultrafiltration—An experimental study, J. Membr. Sci. 242 (2004) 117–128.
[25] C.K. Lee, W.G. Chang, Y.H. Ju, Air slugs entrapped cross-flow filtration of bacterial suspensions, Biotechnol. Bioeng. 41 (1993) 525–530.
[26] T.W. Cheng, Influence of inclination on gas-sparged cross-flow ultrafiltration through an inorganic tubular membrane, J. Membr. Sci. 196 (2002) 103–110.
[27] C. Prabhavathy, S. De, Modeling and transport parameters during nanofiltration of degreasing effluent from a tannery, Asia-Pac. J. Chem. Eng. 6 (2011) 101–109.
[28] R.K. Trivedi, P.K. Goel, Chemical and Biological Methods for Water Pollution Studies, 2nd ed., Environmental Publications, Karad, 1986.
[29] B. Sarkar, S. Pal, T.B. Ghosh, S. De, S. DasGupta, A study of electric field enhanced ultrafiltration of synthetic fruit juice and optical quantification of gel deposition, J. Membr. Sci. 311 (2008) 112–120.
[30] G. Qian, J. Zhou, J. Zhang, C. Chen, R. Jin, W. Liu, Microfiltration performance with two-phase flow, Sep. Purif. Technol. 98 (2012) 165–173.
[31] J.P. Nywening, H. Zhou, Influence of filtration conditions on membrane fouling and scouring aeration effectiveness in submerged membrane bioreactors to treat municipal wastewater, Water Res. 43 (2009) 3548–3558.
[32] S. Pal, S. Ambastha, T.B. Ghosh, S. De, S. DasGupta, Optical evaluation of deposition thickness and measurement of permeate flux enhancement of simulated fruit juice in presence of turbulence promoters, J. Membr. Sci. 315 (2008) 58–66.